Dosimetric characterization of a large area pixel-segmented ionization chamber

S. Amerio
A.O.S. Giovanni Battista, Presidio S. Giovanni A.S., Via Cavour 31, I-10100 Torino, Italy

A. Boriano
Dipartimento di Fisica Sperimentale and INFN, Via P. Giuria 1, I-10125 Torino, Italy

F. Bourhaleb
Dipartimento di Fisica Sperimentale and INFN, Via P. Giuria 1, I-10125 Torino, Italy and Fondazione TERA, Via Puccini 1, I-28100 Novara, Italy

R. Cirio[a)]
Dipartimento di Fisica Sperimentale and INFN, Via P. Giuria 1, I-10125 Torino, Italy

M. Donetti
Dipartimento di Fisica Sperimentale and INFN, Via P. Giuria 1, I-10125 Torino, Italy and Fondazione TERA, Via Puccini 1, I-28100 Novara, Italy

A. Fidanzio
Istituto di Fisica, Università Cattolica S.C. di Roma, Largo F. Vito 1, I-00168 Roma, Italy

E. Garelli
Dipartimento di Fisica Sperimentale and INFN, Via P. Giuria 1, I-10125 Torino, Italy and ASP, Viale S. Severo 65, I-10125 Torino, Italy

S. Giordanengo
Dipartimento di Fisica Sperimentale and INFN, Via P. Giuria 1, I-10125 Torino, Italy

E. Madon
A.O. O.I.R.M. S. Anna, C.so Spezia 60, I-10126 Torino, Italy

F. Marchetto
Dipartimento di Fisica Sperimentale and INFN, Via P. Giuria 1, I-10125 Torino, Italy

U. Nastasi
A.O.S. Giovanni Battista, Presidio S. Giovanni A.S., Via Cavour 31, I-10100 Torino, Italy and Dipartimento di Fisica Sperimentale and INFN, Via P. Giuria 1, I-10125 Torino, Italy

C. Peroni
Dipartimento di Fisica Sperimentale and INFN, Via P. Giuria 1, I-10125 Torino, Italy

A. Piermattei
Istituto di Fisica, Università Cattolica S.C. di Roma, Largo F. Vito 1, I-00168 Roma, Italy

C. J. Sanz Freire[b)]
Dipartimento di Fisica Sperimentale and INFN, Via P. Giuria 1, I-10125 Torino, Italy

A. Sardo and E. Trevisiol
A.O. O.I.R.M. S. Anna, C.so Spezia 60, I-10126 Torino, Italy

(Received 12 August 2003; revised 9 October 2003; accepted for publication 19 November 2003; published 28 January 2004)

A pixel-segmented ionization chamber has been designed and built by Torino University and INFN. The detector features a 24×24 cm^2 active area divided in 1024 independent cylindrical ionization chambers and can be read out in 500 μs without introducing dead time; the digital charge quantum can be adjusted between 100 fC and 800 fC. The sensitive volume of each single ionization chamber is 0.07 cm^3. The purpose of the detector is to ease the two-dimensional (2D) verifications of fields with complex shapes and large gradients. The detector was characterized in a PMMA phantom using ^{60}Co and 6 MV x-ray photon beams. It has shown good signal linearity with respect to dose and dose rate to water. The average sensitivity of a single ionization chamber was 2.1 nC/Gy, constant within 0.5% over one month of daily measurements. Charge collection efficiency was 0.985 at the operating polarization voltage of 400 V and 3.5 Gy/min dose rate. Tissue maximum ratio and output factor have been compared with a Farmer ionization chamber and were found in good agreement. The dose profiles have been compared with the ones obtained with an ionization chamber in water phantom for the field sizes supplied by a 3D-Line dynamic multileaf collimator. These results show that this detector can be used for 2D dosimetry of x-ray photon beams, supply-

ing a good spatial resolution and sensibly reducing the time spent in dosimetric verification of complex radiation fields. © *2004 American Association of Physicists in Medicine.*
[DOI: 10.1118/1.1639992]

Key words: dosimetric characterization, 2D ionization chamber array, radiation therapy quality assurance

INTRODUCTION

Modern conformational external radiotherapy with photon beams takes advantage of fast computers, sophisticated algorithms and precise mechanics to get closer to the goal of concentrating the damage on the tumor while sparing healthy tissue. As a drawback, verification and safety issues may become extremely cumbersome and crucial.[1,2] Techniques making use of multileaf collimators achieve a very good conformation of dose distributions with high gradient fields that can change with time as intensity modulated radiotherapy.[3] A detector realized with a segmented ionization chamber has been developed to allow two-dimensional (2D) radiation measurement in real time. A detector with similar design has shown good results in the dosimetry of hadron and electron beams;[4,5] in this paper a detailed description of the detector and the results of its dosimetric characterization are presented for photon beams. With respect to other kind of systems such as parallel plate flatness monitors,[6,7] liquid ionization chamber arrays,[8,9] electronic portal imaging devices,[10] silicon diode arrays,[11] and matrices[12] this detector has several advantages: granularity, spatial resolution, fast and dead time free readout, high dose rate capability, stability, resistance to radiation.

MATERIALS AND METHODS

Chamber design and construction

The detector is a pixel-segmented ionization chamber (PXC), whose main features are 2D readout capability, large detection area, good homogeneity and dead time free readout. A similar architecture has been successfully tested on hadron and electron beams.[4,5] The whole chamber is made of Plexiglas and very thin layers of aluminum and copper. A total of 1024 detectors are distributed on a $24\times24\ \mathrm{cm}^2$ area.

The chamber can be seen in Fig. 1, that shows the central part (sensitive area) and the four blue covers hiding the readout electronics. Figure 2 gives a schematic view of the chamber, where the two planar electrodes mounted on square Plexiglas plates can be seen. It must be noted that, for graphical reasons, the pattern drawn on the anode is different from the actual one, having 14×14 pixels instead of 32×32. The cathode is an aluminized Mylar foil. The anode consists of a foil of glass fiber tissue embedded in epoxy (commercially known as Vetronite) sandwiched between two thin layers of copper. By using the standard printed circuit board (PCB) technique we obtained 32×32 square conductive pixels, 7.5 mm wide, on one side of the Vetronite foil; the 100 μm tracks connecting each pixel to the output connector and the electronics boards lay on the opposite side of the foil and were covered by a thin layer of nonconductive paint to avoid cross talk and contribution from charges created outside the fiducial volume.

The anode and cathode foils are fixed to 5 mm thick Plexiglas plates. An additional 5.5 mm thick Plexiglas plate, with 1024 holes, is placed between anode and cathode. The diameter of each hole is 4 mm. The plates are not sealed, thus the air volume inside each chamber communicates with the outside.

In summary the detector consists of a 32×32 matrix of 1024 cylindrical ionization chambers arranged in a square of $24\times24\ \mathrm{cm}^2$ area. Each chamber has a 4 mm diameter and

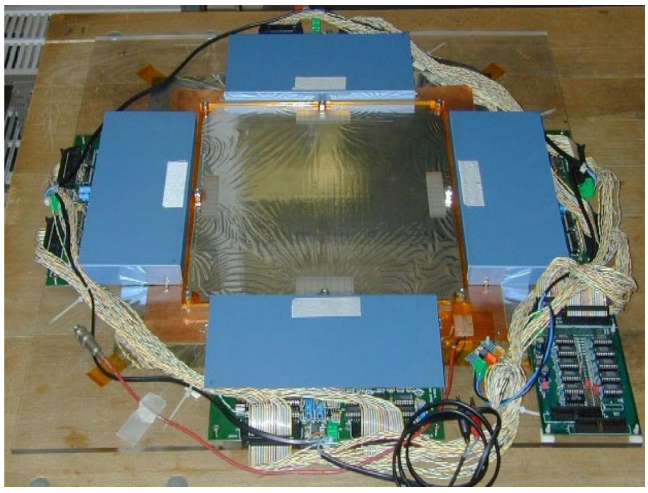

FIG. 1. The pixel-segmented ionization chamber (PXC).

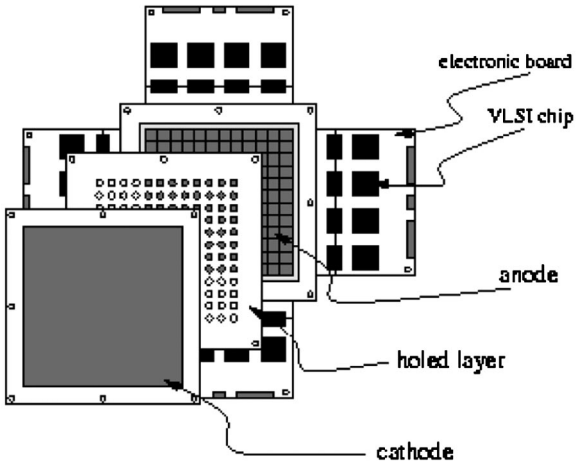

FIG. 2. Exploded view of the PXC.

5.5 mm height, the center at a distance of 7.5 mm from the center of the next one. The sensitive volume of each single ionization chamber is about 0.07 cm^3.

The overall area of the PXC is 650×650 mm^2, while the dimension along the beam axis is about 20 mm.

The typical high voltage working value is -400 V. A passive low-pass filter is used to filter the high frequencies picked up from the high voltage cable.

Front end read out and data acquisition

The design of the front end is based on the recycling integrator architecture.[13] Briefly, the input current from each pixel is integrated and a number of pulses proportional to the charge collected by an individual pixel are sent to a 16-bit counter. An ensemble of 64 channels has been integrated in a single very large scale integration (VLSI) chip.[14]

At any given time all the counters can be latched and the results are stored on a register. This is like taking a snapshot of the charges collected by the 1024 pixels. The relevant features of the front end circuit are summarized below.

(i) The charge corresponding to a pulse (charge quantum) can be adjusted between 100 fC and 800 fC via an externally regulated voltage. In fact the charge is generated with a pulse loading a 200 fF capacitor, which is then discharged on the integrator itself.
(ii) Maximum pulse frequency is 5 MHz which results in a limit for the pixel input current of 4 μA for a charge quantum set at 800 fC.
(iii) Linearity from 100 pA up to the maximum current is within 1%.
(iv) Dark current counting rate is at the level of ~1 Hz.
(v) Charge quantum spread is less than 1%.
(vi) The change of charge quantum as function of temperature in the range 20 °C–30 °C is less than 1 fC/°C for a charge quantum at 600 fC.
(vii) Polarization voltage of the chip is $+5$ V.
(viii) No dead time is introduced during readout because the charge quantum is subtracted from the integrator input as the current from the detector flows in and the latch located at the output of the counters does not affect the counting itself.

The VLSI chip has to be kept outside the radiation field because, though radiation damage is not a concern,[15] it responds to radiation approximately the same way as the PXC itself. Contribution to the counting due to stray radiation has been measured with fields of several dimensions (in the range 5×5 to 10×10 cm^2) and resulted below 0.2%.

The bus between front end cards and data acquisition includes, besides the 16 data lines, 10 address lines to multiplex 1024 pixels. Furthermore an analog reset to discharge the integrator capacitor at the beginning of the operations, a digital reset to clear all the counters, and a strobe to latch them are necessary.

The data acquisition system is based on a National Instruments (NI) fast input/output 32-bit digital PCI card mounted on a computer hosting the LabView software.

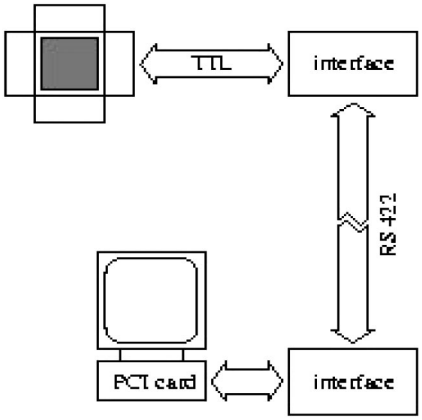

FIG. 3. Block diagram of the data acquisition system.

The TTL signal logic used on the front end and NI cards does not allow driving long lines; thus two interface cards have been designed and built to transform all the TTL digital signals into RS-422 (differential TTL). Two flat 34-lead cables up to 200 m long connect the front end card and the computer hosted NI card.

Figure 3 shows a block diagram of the data acquisition system. A read out cycle for the 1024 pixels may take a time as short as 500 μs; it must be noted that for most applications a readout rate of 1 Hz is sufficient and does not flood with data the read out computer.

The same system allows online display of the 1024 signals and data storage on disk. While online display can be performed with a maximum refresh rate of 1 Hz, data storage can be performed at full speed taking advantage of the memory located on the NI read out board. A sample display of the computer monitor during a typical data taking session is shown in Fig. 4. The parameters checked in this case were the 2D distributions of counts integrated over the last second and the 2D accumulated charge, displayed every second.

Dosimetric characterization

The dosimetric characterization of the PXC was carried out using PMMA layers placed upstream of the PXC to obtain different water equivalent depths. Backscattering effect was taken into account placing a thickness of 4.0 cm of PMMA downstream of the PXC.

A method to intercalibrate the pixels has been implemented; it sets no request on the beam, which can have any dimension and any shape. However, the beam shape must not change during the three subsequent irradiations needed for the calibration. In this way the user can decide to calibrate just the area of PXC needed for the measurement. In our case, for example, we have calibrated the PXC with a 24×24 cm^2 field when working with a ^{60}Co unit and with a 12×12 cm^2 field size when using a 6 MV x-ray photon beam obtained with an Elekta clinical linac equipped with 3D-Line dynamic multileaf collimator.

The calibration procedure is the following.

Step 1: the PXC is centered on the beam axis and irradiated.

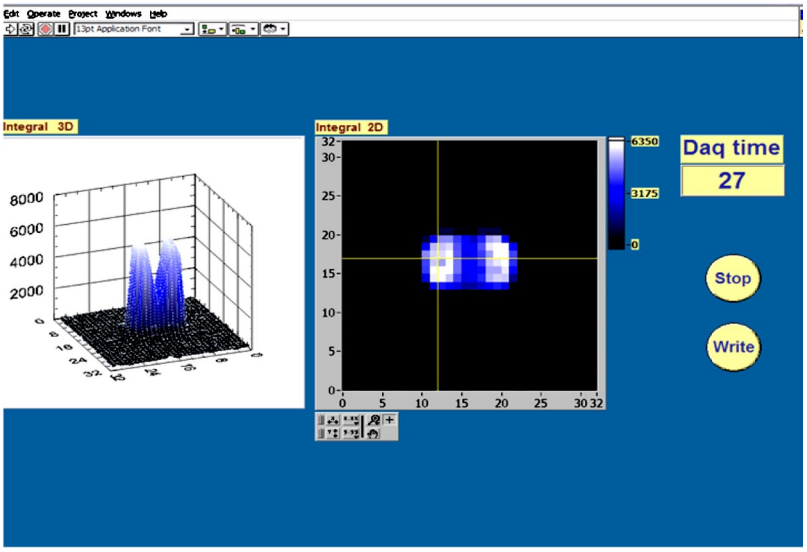

FIG. 4. Computer display during a typical data acquisition session.

Step 2: after a 90° rotation about beam axis, the PXC is irradiated again.

Step 3: finally the PXC is shifted by one pixel (7.5 mm) in cross-plane direction and irradiated for a third time.

After this procedure and applying an appropriate algorithm the pixels are correctly intercalibrated. Using an external dosimeter as reference for one of the pixels, the PXC absolute calibration factor is obtained. All results shown in the following were obtained after applying the calibration procedure mentioned above.

To measure the detector response stability, two different tests have been performed. In one case, the PXC has been irradiated during one month of daily measurements at a ^{60}Co irradiation facility, taking great care to avoid any mechanical stress to the PXC detector, in order not to modify the distance between anode and cathode. In a second test, the PXC has been used in three different hospitals, with three different accelerators over a 7 month period; moreover, for servicing purposes, during this period the PXC has been disassembled and reassembled several times. With ^{60}Co beam, tests were done at a water equivalent depth of 1.2 cm with a field size of 24×24 cm^2. The linear accelerators were an Elekta SL 75-5, a Siemens Primus and a Varian CLINAC 610 CD with 6 MV 24×24 cm^2 photon beam at maximum dose equivalent water depth.

A 6 MV photon beam of an Elekta SL 75-5 clinical accelerator, collimated with an additional 3D-Line multileaf collimator with 2×20 leaves, 6.2 mm wide at isocenter, was used for the PXC dosimetric characterization. The 3D-Line collimator supplied square fields up to 12×12 cm^2.

A Farmer-type ionization chamber Capintec PR06C, with a sensitive volume of 0.65 cm^3, a 6.4 mm inner diameter, polarized at a bias voltage of $+300$ V was connected to a Capintec electrometer, model 192, and used as a reference dosimeter to determine the dose and the dose rate to water along the central beam axis following the AAPM TG-51[16] code of practice.

The dosimetric characterization of the PXC was carried out in terms of linearity with dose in the range 0.1–10 Gy and in terms of linearity with dose rate selecting four points (0.74, 1.5, 3.0, 6.12 Gy/min) obtained changing the Elekta linac pulse repetition frequency. These measurements were performed with a 10×10 cm^2 field size at maximum dose equivalent water depth ($d_{max}=1.5$ cm) by placing PMMA layers upstream of the PXC.

The tissue maximum ratio (TMR) has been measured with the 6 MV photon beam at different water equivalent depths. PMMA layers were placed upstream of the PXC and the effective point of the PXC, that is half-way between anode and cathode, was placed at isocenter, at 100 cm Source Axis Distance (SAD). The TMR data obtained with the PXC were compared with the same data obtained by the PR06C ionization chamber.

The output factor (OF), defined as the central pixel reading normalized at the field size of 10×10 cm^2, was determined using the PXC and the Farmer chamber at d_{max} of the 6 MV x-ray beam.

The relative dose profiles measured with the PXC and a water phantom, on a 6 MV x-ray beam at the field size of 10×10 cm, were compared. Scan of beam profiles were made with a three-dimensional water phantom system (PTW, Freiburg, Germany). Scans were made with a cylindrical ionization chamber, model 31002, which had a 0.125 cm^3 volume and a diameter of the sensitive area of 5.5 mm, connected to a PTW Tandem dual channel electrometer (10015).

For all measurements the effective points for the ion chambers (PXC, Farmer and PTW 31002) were placed at isocenter and the SAD were 80 cm for ^{60}Co and 100 cm for Elekta linac.

The uncertainty of the experimental data is the statistical variation observed over the measurement values and resulted 0.5% for all measurements. In the following, error bars are shown only when the symbol dimensions are smaller than experimental uncertainty.

All data have been corrected for temperature and pressure variations.

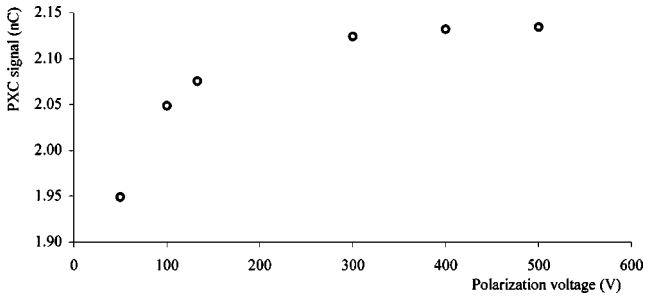

FIG. 5. Sum of the four central pixels reading as a function of polarization voltage obtained at 3.5 Gy/min.

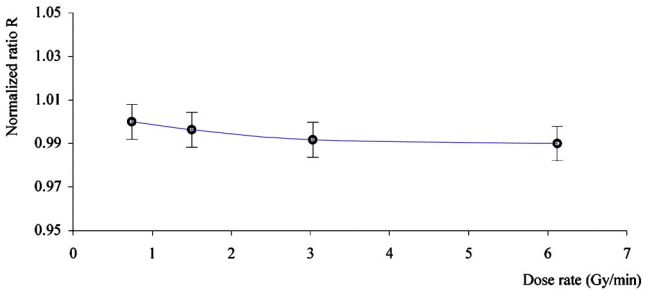

FIG. 7. Normalized ratio R between PXC and PR06C current as a function of dose rate to water for a 6 MV x-ray beam.

RESULTS AND DISCUSSION

Detector response stability

The signal reproducibility of the PXC has been tested during one month of daily measurements at a ^{60}Co irradiation facility and it was found constant within 0.5% (1σ). In addition, the stability of the PXC response was measured over a 7 months period. Repeating the calibration in three different Hospitals with three different 6 MV accelerators, the relative variation in the chamber response was 1.3% (1σ). As a comment to this value, one has to take into account that during the period in which the tests were performed the chamber has been moved and dismounted several times. The quoted value can then be considered an upper limit for the variation of chamber response. There is no evidence for any dependence on time or integral dose. The sensitivity measured at $d_{\max}$ with a 6 MV beam was 2.1 nC/Gy.

Collection efficiency

The readings of the PXC in terms of collected charge (in nC) were studied as a function of the polarization voltage to determine the optimum working point. Figure 5 shows the sum of the four central pixel reading obtained as a function of the polarization voltage with a 6 MV x-ray beam at $d_{\max}$. At this depth the dose rate was of 3.5 Gy/min. The difference in collected charge in the range 400–500 V was 0.1%.

The same measurements were performed also at 5.0 cm and 10.0 cm equivalent water depths. The relative difference between the readings obtained at 400 V and 500 V were less than 0.1%. The polarization voltage equal to 400 V for the PXC was selected.

Using the two-voltage method[16–18] a collection efficiency varying between 0.985 and 0.988 respectively for $d_{\max}$ and 10 cm water depth was found.

Dose and dose-rate dependence

The response of the PXC with respect to charge buildup and integral dose has been verified by exposing it to several doses. In Fig. 6 the behavior of the detector in the range 0.1–10 Gy is shown, where the linear correlation coefficient R^2 was found to be equal to 1.000.

To evaluate the dose-rate linearity, the ratio R between the charges measured with PXC and PR06C at the same $d_{\max}$ depth was determined. Figure 7 shows the above ratios normalized at 0.74 Gy/min as a function of the dose rate to water.

The average value of the PXC background was 1.1 ± 0.05 counts/s, to be compared with ~ 1000 counts/s at $d_{\max}$ for a dose rate of 3 Gy/min.

Tissue maximum ratio, output factor, and beam profile measurements

Figure 8 shows the TMR data obtained with a 12×12 cm^2 field size with the PXC compared with the same data obtained with a Farmer chamber. The results are in agreement better than 0.4%, well within the 0.5% experimental uncertainty.

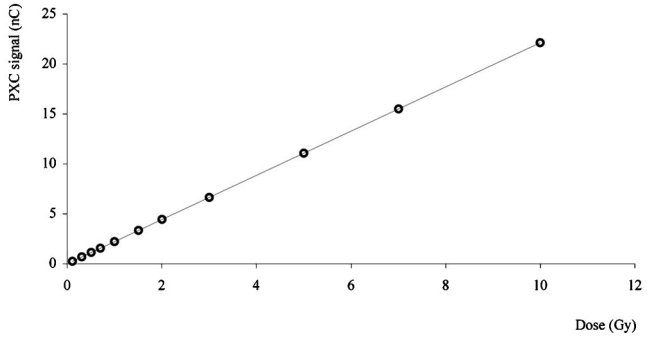

FIG. 6. Average reading of the four central pixels of the PXC as a function of the absorbed dose to water determined at $d_{\max}$.

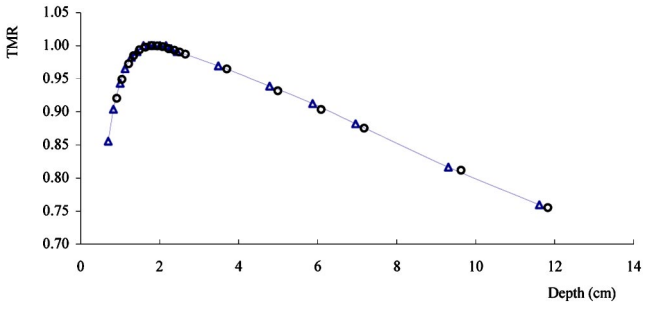

FIG. 8. TMR data obtained with a 12×12 cm^2 field of a 6 MV x-ray beam, using a Farmer chamber (△) and the PXC (○).

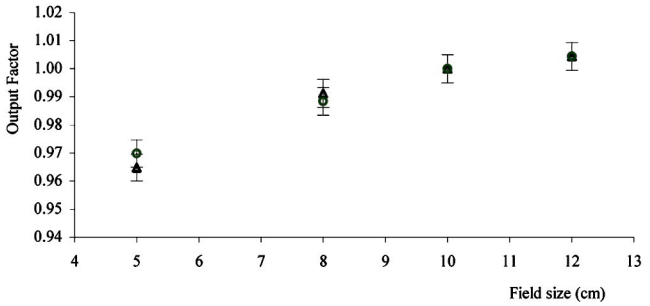

FIG. 9. Output factor data obtained for a 6 MV x-ray beam at d_{max} using a Farmer chamber (△) and the PXC (○).

The output factor response results measured by the PXC and the PR06C ion chamber are presented in Fig. 9 for different field sizes varying from 5×5 cm^2 to 12×12 cm^2. The results show differences smaller than 1%, however within the experimental uncertainty 0.5%.

Figure 10 shows the comparison between the beam profiles obtained in a water phantom with the PXC and with an ionization chamber, for a 10×10 cm^2 field size at d_{max}, normalized on the beam central axis. Data are in agreement on the flat top, in the penumbra region and in the tail region. The three regions are related to different contributions: the flat top is strongly dominated by the intercalibration of the 1024 chambers. As previously described, the PXC has been calibrated using a method independent from the beam shape and here the effectiveness of the calibration can be appreciated. In the penumbra region, the volume in which the measurement is performed is important. In our case each one of the 1024 individual chambers in the PXC has a 0.07 cm^3 volume and a 4 mm diameter that is small enough to accurately measure the profile, as long as the field size is not smaller than 4×4 cm^2. Further tests are needed to verify the response of the detector with smaller fields. In the tail region the PXC measurement is in good agreement with the water phantom results, which means that, despite the large number of channels readout in parallel, there is no measurable cross talk.

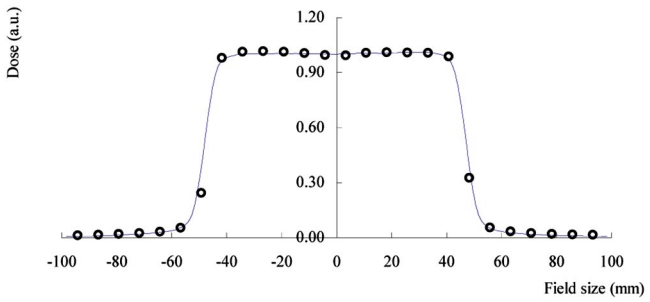

FIG. 10. Comparison of beam profiles measured with an ionization chamber in a water phantom (—) and with the PXC (○). The irradiations were performed in a MV x-ray beam at d_{max} and 10×10 cm^2 field size. The results are normalized to the central beam axis.

CONCLUSIONS

A pixel-segmented ionization chamber has been designed and built by Torino University and INFN. It features a 24×24 cm^2 active area divided in 1024 separately readout cylindrical ionization chambers (pixels) 4 mm diameter and 5.5 mm height, with a 7.5 mm pitch. The whole chamber can be readout in 500 μs without introducing dead time in the measurement and the digital charge quantum can be adjusted between 100 fC and 800 fC. The sensitive volume of each single ionization chamber is 0.07 cm^3.

The dosimetric characterization of the PXC has been performed in a PMMA phantom using ^{60}Co and 6 MV x-ray photon beams. The PXC has shown good signal linearity with respect to dose and dose-rate to water. The average sensitivity was 2.1 nC/Gy, constant within 0.5% over one month of daily measurements. Charge collection efficiency was 0.985 at a polarization voltage of 400V for a 3.5 Gy/min dose rate.

Tissue maximum ratio and output factor determined with the PXC were in agreement with the ones obtained by Farmer ionization chamber. A good agreement was also observed between the dose profiles obtained with an ionization chamber in a water phantom and the PXC for the field sizes supplied by the 3D-Line dynamic multileaf collimator.

A similar version of PXC has been tested in the past as dosimeter of hadron and electron beams;[4,5] in the present paper it is shown that the PXC can be used for conventional 2D x-ray beam dosimetry too.

The good spatial resolution over a large area shown by the PXC can sensibly reduce the time spent in dosimetric verification of complex radiation fields.

ACKNOWLEDGMENTS

The authors thank Dr. Igor Gomola for performing the dose linearity data taking. S.G. and C.J.S.F. were partially supported by Wellhöfer/Scanditronix, Bahnhofstr. 5, D-90592 Schwarzenbruck, Germany.

[a]Author to whom correspondence should be addressed; electronic mail: cirio@to.infn.it
[b]Present address: Hospital Universitario de Salamanca, Paseo de San Vicente 182, Salamanca, Spain.

[1] S. Webb, *The Physics of Conformal Radiotherapy* (IOPP, Bristol, 1997).
[2] S. Webb, *Intensity Modulated Radiation Therapy* (IOPP, Bristol, 2000).
[3] AAPM Report 72, Basic Applications of Multileaf Collimators: Report of the AAPM Radiation Therapy Committee Task Group No. 50 (Medical Physics Publishing, 2001).
[4] C. Brusasco *et al.*, "Strip ionization chambers as 3-D detector for hadrontherapy," Nucl. Instrum. Methods Phys. Res. A **389**, 499–512 (1997).
[5] S. Belletti *et al.*, "Performances of a pixel ionization chamber with electron beams," Physica Medica—Vol. XV, N.3, July–September 1999.
[6] E. Martell *et al.*, "A flatness and calibration monitor for accelerator photon and electron beams," Int. J. Radiat. Oncol., Biol., Phys. **12**, 271–275 (1986).
[7] B. R. Paliwal *et al.*, "A consistency monitor for radiation therapy treatments," Med. Phys. **23**, 1805–1807 (1996).
[8] H. H. Liu *et al.*, "Measuring dose distributions for enhanced dynamic wedges using a multichamber detector array," Med. Phys. **24**, 1515–1519 (1997).
[9] C. Martens *et al.*, "The value of the LA linear ion chamber array for characterization of intensity-modulated beams," Phys. Med. Biol. **46**, 1131–1148 (2001).

[10] K. L. Pasma *et al.*, "Dosimetric verification of intensity modulated beams produced with dynamic multileaf collimation using an electronic portal imaging device," Med. Phys. **26**, 2373–2378 (1999).
[11] T. C. Zhu *et al.*, "Performance evaluation of a diode array for enhanced dynamic wedge dosimetry," Med. Phys. **24**, 1173–1180 (1997).
[12] P. A. Jursinic *et al.*, "A 2-D diode array and analysis software for verification of intensity modulated radiation therapy delivery," Med. Phys. **30**, 870–879 (2000).
[13] B. Gottschalk, "Charge-balancing current integrator with large dynamic range," Nucl. Instrum. Methods Phys. Res. A **207**, 417–421 (1983).
[14] G. C. Bonazzola *et al.*, "Performances of a VLSI wide dynamic range current-to-frequency converter for strip ionization chambers," Nucl. Instrum. Methods Phys. Res. A **405**, 111–120 (1998).
[15] F. Bourhaleb *et al.*, "Radiation damage studies of a recycling integrator VLSI chip for dosimetry and control of therapeutical beams," Nucl. Instrum. Methods Phys. Res. A **482**, 752–760 (2002).
[16] "AAPM TG-51 protocol for clinical reference dosimetry of high-energy photon and electron beams," Med. Phys. **26**, 1847–1870 (1999).
[17] J. W. Boag, "The recombination correction for an ionization chamber exposed to pulsed radiation in a 'swept beam' technique," Phys. Med. Biol. **27**, 201–211 (1982).
[18] ICRU Report 34, "The dosimetry of pulsed radiation," 1982.